EQUIVALENT ELECTRICAL CIRCUIT FOR DESIGNING MEMS-CONTROLLED REFLECTARRAY PHASE SHIFTERS

F. A. Tahir and H. Aubert

LAAS-CNRS and University of Toulouse
UPS, INSA, INP, ISAE
F-31077 Toulouse, Ave. du colonel Roche 7, Toulouse, France

E. Girard

Research Department
Thales Alenia Space
F-31037 Toulouse, France

Abstract—This article presents an equivalent electrical circuit for designing Radio-Frequency MEMS-controlled planar phase shifter. This kind of phase shifters has recently been incorporated in reconfigurable reflectarrays. The proposed equivalent circuit depends on the number, the ON/OFF state and the locations of the switches inside the unit cell. Such equivalent circuit is used for determining, with a little computational effort, the two important design parameters i.e., the number and the locations of RF-MEMS switches in the phase shifter cell. These two design parameters then allow a designer to design a phase shifter cell having a linear distribution of a given number of phases over 360° phase range at a single desired frequency.

1. INTRODUCTION

Electronically tunable microstrip reflectarrays are getting more and more attraction and significance these days and are successfully being applied in electronically scanning and beam-steering antennas [1–3]. These reconfigurable reflectarrays possess the advantages of both fixed beam reflectarrays (such as small size, less weight and low cost) and active phased arrays (e.g., beam scanning, adaptive radiation pattern and dynamic phase control). These attributes

---

Corresponding author: F. A. Tahir (fatahir@laas.fr).

have made them in recent years an excellent antenna technology especially for satellite applications [4]. However, the above mentioned benefits are at the cost of high complexity in the reconfigurable microstrip reflectarray antenna structures. This complexity, in turn, becomes a severe handicap performing the analysis and design of such reconfigurable reflectarrays. Though, for such complex reflectarray antenna structures, the conventional numerical methods provide a comprehensive analysis capable of giving frequency details and polarization responses, they often require lengthy CPU-time, a lot of memory, and consequently fail to provide efficient tools especially for designing and optimization purposes [5, 6].

To offer an electromagnetic (EM) model for such structures that could be useful for designers, equivalent circuit approaches can be applied. Recently, an equivalent circuit [7] based on the transmission line model is presented to analyze the scattering behavior of an electronically tunable varactor-based unit cell; however this model cannot be used as a dynamic design tool as the number of command elements and their position is fixed.

In this letter, for the first time, an equivalent circuit model is presented to design a phase shifter cell electronically tunable by MEMS switches. The phase shifters of this kind have recently been developed and used in reconfigurable reflectarrays [4, 8]. This equivalent circuit depends on the number, the ON/OFF state and the locations of the MEMS inside the phase-shifter cell. Moreover the circuit model has been used for determining, with a little computational effort, the locations and the minimum number of the MEMS that allow synthesizing a uniform distribution of a given number of phases at a single desired frequency within the operating frequency band.

The paper is organized as follows: Section 2 describes the methodology for the extraction of the equivalent circuit and Section 3 explains how the equivalent circuit is used as a design and optimization tool for determining such phase shifter configurations which allow synthesizing a uniform distribution of a given number of phases. The conclusion is drawn in Section 4.

2. EQUIVALENT ELECTRICAL CIRCUIT MODEL

2.1. Geometry of the Problem

A complete schematic diagram of the phase shifter cell loaded with MEMS switches is shown in Fig. 1. All the details of the unit cell are given in the caption.

In the arrangement shown in Fig. 1, the transverse electromagnetic mode (TEM) is the only one propagating mode within the operating
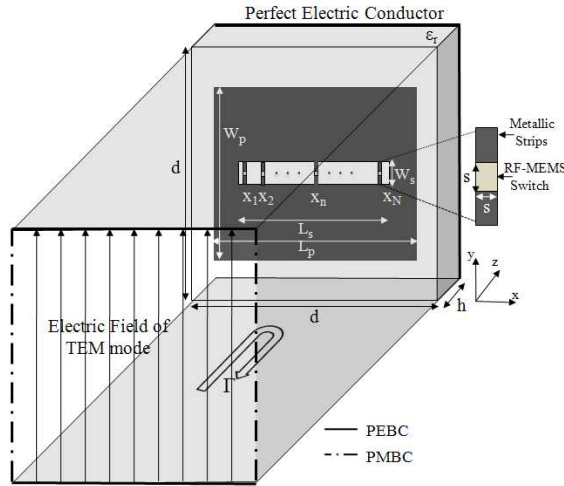
Figure 1. The phase-shifter cell in the TEM-mode waveguide: $d = 12\,\text{mm}$, $L_p = 9\,\text{mm}$, $W_p = 6\,\text{mm}$, $L_s = 7\,\text{mm}$, $w_s = 0.75\,\text{mm}$, $S = .01\,\text{mm}$, $h = 1.5\,\text{mm}$ and $\varepsilon_r = 2.9$. MEMS switch is modeled by equivalent surface impedance. The number of switches in the slot is denoted by N while x_n $(n = 1, 2, \ldots, N)$ refers to the coordinate of the n-th switch in the slot. Metallic strips connect the switches to the patch. PEBC and PMBC stand for Perfect Electric and Perfect Magnetic Boundary Conditions respectively.

frequency band. The number N and the locations $x_1, x_2, x_3, \ldots, x_N$ of the switches depend on the design requirements. The reflectarray phase shifter cell is placed at the end of a waveguiding structure of transverse dimensions $d \times d$. The phase shift applied to the TEM mode when reflecting from the cell is assumed to be identical to that experienced by a plane wave electric field incident on a given cell [7]. The estimation of this phase shift or equivalently the phase of the reflection coefficient Γ through a simple equivalent circuit model is now presented. The dielectric and metallic losses are not taken into account in the present analysis.

2.2. Methodology for the Extraction of the Equivalent Electrical Circuit

The equivalent circuit is derived from step by step approach. First, in the set of Fig. 1, replace the patch loaded with slot and MEMS by a simple metallic patch having the same dimensions $W_p \times L_p$. Full-wave EM simulations of this simple patch indicate that the two first resonant modes, i.e., the TM_{01} and TM_{21}, contribute significantly to

the value of the phase of the reflection coefficient within the frequency range of interest (DC to $14\,\mathrm{GHz}$). The equivalent circuit of this simple patch is then given by two LC-series circuits (L_1C_1 and L_2C_2 as shown in the Fig. 4) connected in parallel and shunted by a short-circuited transmission line. One LC-series circuit is associated with one resonant mode and the short-circuited transmission line models the dielectric slab of thickness h metalized on one side. The characteristic impedance of this line is $Z_c = Z_0/\sqrt{\varepsilon_r}$, where Z_0 denotes the free-space wave impedance and ε_r is the relative permittivity of the dielectric slab, the propagation constant β of the fundamental TEM-mode is $k_0\sqrt{\varepsilon_r}$ where k_0 is the free-space wave-number.

From the above simulation results, the numerical values of the circuit elements L_1, C_1, L_2 and C_2 can be derived as follows: (1) at $11.4\,\mathrm{GHz}$ and $22.8\,\mathrm{GHz}$, the phase of the reflection coefficient is found to be zero, i.e., the equivalent circuit resonates at these frequencies turning the equivalent admittance to zero (2) at $16\,\mathrm{GHz}$ and $24.75\,\mathrm{GHz}$, this phase is found to be π, i.e., the equivalent circuit impedance becomes zero. From these two simulation results, a system of four independent equations combining the four unknowns (L_1, C_1, L_2 and C_2) is formulated and solved. The results are reported in Table 1.

Now load this patch with the slot. It was observed on the basis of the simulation results (not reported in this paper) that the phase of the reflection coefficient can be accurately predicted within the frequency band of interest by connecting an LC-parallel circuit (L_sC_s) in series with the just derived simple patch circuit model as shown in the Fig. 4. The values of L_s and C_s can be deduced by following two conditions: (1) at $10.4\,\mathrm{GHz}$ the phase of the reflection coefficient is found to be π (i.e., the equivalent circuit impedance is zero) and (2) at $18.45\,\mathrm{GHz}$ the phase is found to be zero (i.e., this frequency is the resonant frequency for the structure). Applying these two conditions one can reach the values of L_s and C_s (see Table 1).

Table 1. Values of the elements L_1, C_1, L_2, C_2, L_s and C_s appearing in the equivalent circuit of Fig. 4.

C_1 (pF)	C_2 (pF)	L_1 (nH)	L_2 (nH)	C_s (pF)	L_s (nH)
0.04	0.01	2.41	4.79	1.58	0.06

Owing to brevity, the mathematical manipulations during the 1st and 2nd steps are not presented in this letter but the final phase results in case of simple patch and patch loaded with slot obtained by equivalent circuit models and HFSS are shown in Figs. 2(a) and 2(b) respectively. The circuit results are in excellent agreement with the results of full-wave EM simulation.
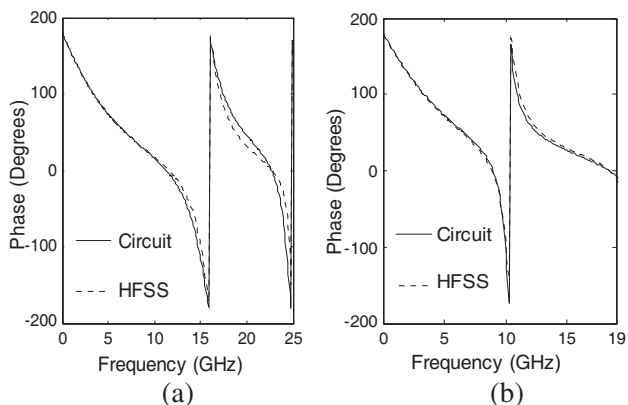
Figure 2. Equivalent circuit and HFSS results for: (a) Patch structure only, (b) patch loaded with slot.
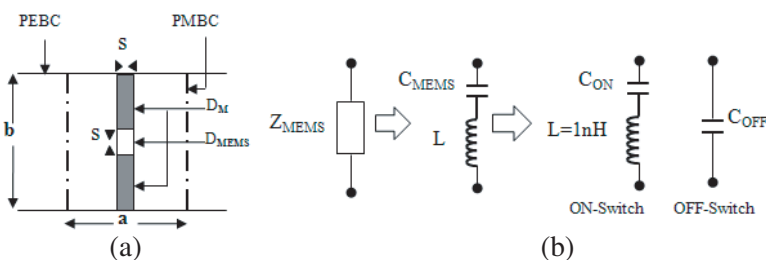
Figure 3. (a) MEMS and its connections to the patch, (b) equivalent circuit model when the MEMS switch is located at the center of the slot.

Next, load the slot *at its centre* by a single capacitive RF-MEMS switch. A capacitive MEMS switch generally has ON-state (C_{ON}) and OFF-state (C_{OFF}) capacitances in between 1–4 pF and 20–50 fF [9, 10] respectively. Moreover the typical loss resistance of such MEMS is in between $0.1\,\Omega$ and $1\,\Omega$ (if such resistance is connected in series with the MEMS capacitance in the equivalent circuit, we observed that the phase diagram of the reflectarray element remains same as obtained in the lossless case). To model the MEMS including its connections, consider the MEMS *at the centre* of the slot denoted by the domain D_{MEMS} and the connections denoted by the domain D_M as shown in Fig. 3(a).

The MEMS and its connections can be modeled by purely reactive impedance Z_{MEMS} as shown in Fig. 3(b), where C_{MEMS} (C_{ON} or C_{OFF}) designates the ON/OFF capacitance of the MEMS and L denotes the inductance of the domain $D_{MEMS} \cup D_M$. This inductance

can be estimated by the following equation.

$$L = \mu_0 \frac{b}{a} \sum_{n=1,2,3,\ldots}^{\infty} \frac{1}{\sqrt{(2n\frac{\pi}{a})^2 - k_0{}^2}} \text{sinc}^2 \left(n\frac{\pi}{a}s\right) \qquad (1)$$

where b and s denote respectively the width of the slot and the strip. This approximation is derived from the application of the Integral Equation Technique using entire domain trial functions (for a description of this technique see, e.g., [11]). For deriving Equation (1) a uniform trial function has been used for expanding the current density in the domain $D_{MEMS} \cup D_M$ and a uniform trial function has been adopted for describing the tangential electric filed in D_{MEMS}. In our application, $s = 100\,\mu\text{m}$, $a = 7\,\text{mm}$, $b = 750\,\mu\text{m}$ and central frequency is equal to $12.5\,\text{GHz}$.

   The inductance is then found to be close to $1\,\text{nH}$. When the switch is OFF, this inductance can be neglected since $L\omega \ll 1/\omega C_{OFF}$, where $C_{OFF} = 0.04\,\text{pF}$. So the equivalent impedance Z_{MEMS} in this case is close to $1/\omega C_{OFF}$. Moreover, when the switch is ON, the impedance effect of the inductance L is not negligible and the equivalent impedance becomes equal to $\omega L + 1/\omega C_{ON}$ (see Fig. 3(b)). Finally the equivalent circuit model for the phase-shifter cell when *the slot is loaded at its center by single MEMS* is then given in Fig. 4. If the MEMS switch is located *at the edges of the slot*, it is shunted and consequently it does not participate in the phase-shift, i.e., the phase-shift in this case is provided only by the patch and slot. This situation can be modeled simply by removing the impedance Z_{MEMS} from the equivalent model of Fig. 4.
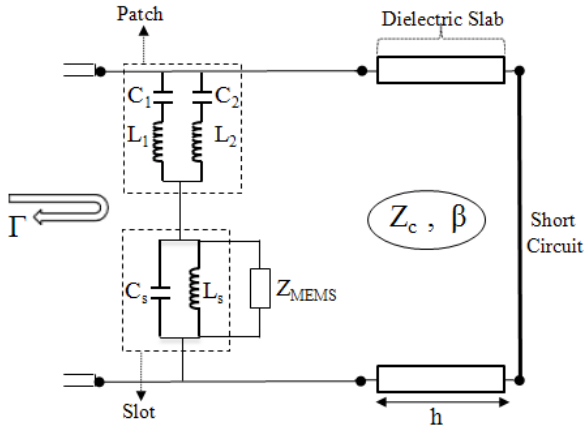
Figure 4. Equivalent electrical circuit for the MEMS-controlled phase-shifter cell, the slot is loaded at its center by single MEMS.
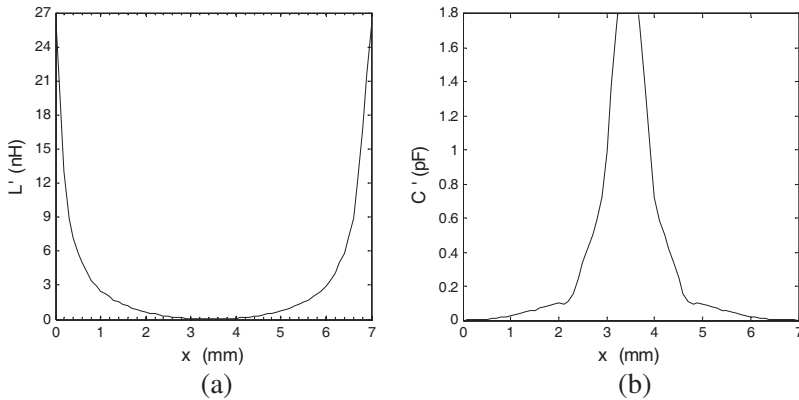
Figure 5. Variations of (a) inductance L' and (b) capacitance C' versus position of a single MEMS switch in the slot.

Now in order to extract an equivalent circuit allowing the modeling of the cell having single MEMS *at an arbitrary location* between the edges and the center of the slot, we propose to connect a position-dependent impedance $Z'(x)$ in series with Z_{MEMS} such that: (1) $Z' = 0$ when the MEMS is at the center of the slot and (2) Z' is infinite when the MEMS is at the edges of the slot. For an arbitrary location x of the MEMS between the edges and the center of the slot, the value of Z' is extracted from full wave simulations.

The physical interpretation (if it exists) of Z' is still under investigation. However, by definition, this artificial impedance allows us to propose an electrical circuit that models a cell having *single MEMS* at an arbitrary location between the edges and the center of the slot. By full-wave simulations, we observe that $Z'(x) = j\omega L'(x)$ when the MEMS is ON while $Z'(x) = 1/j\omega C'(x)$ when the MEMS is OFF. The variations of L' and C' versus the position x of the MEMS are reported in Figs. 5(a) and 5(b) respectively. The corresponding values of L' and C' to a specific position of the MEMS inside the slot have been determined from the circuit simulations such that the phase given by the equivalent circuit is very close to one given by full wave EM simulations. So the overall changing behavior of L' and C' along the length of the slot is obtained by taking 70 different positions of single MEMS inside the slot taking scanning step of 0.1 mm.

To generalize the one MEMS equivalent circuit model of the Fig. 4 for the phase-shifter cell having N (more than one) number of MEMS with coordinates $x_1, x_2, x_3, \ldots, x_N$ as shown in Fig. 1, we simulated the equivalent circuit on ADS taking different number of MEMS from 1 to 9 (with L_1, C_1, L_2, C_2, L_s, C_s and Z' (obtained from Fig. 5)

are those derived in case of single MEMS, i.e., no HFSS simulation involves to find circuit model for a phase shifter cell having more than one MEMS, rather it is derived from already extracted single MEMS model). The results given by the equivalent circuit model are then compared with HFSS and are found to be in a very good agreement. As an illustration, Fig. 7 in the Section 3 gives the results in case of three MEMS.

Ultimately, the equivalent circuit of the phase-shifter cell having N number of MEMS is shown in Fig. 6(a). The elements L_1, C_1, L_2, C_2, L_s, C_s and Z' are those derived in case of single MEMS. The reflection coefficient Γ of the TEM mode when reflecting from the cell is then derived from the expression $\Gamma = (Z_L - Z_{REF})/(Z_L + Z_{REF})$ where $Z_{REF} = 50\,\Omega$ and Z_L denotes the impedance of the one-port shown in Fig. 6(a).
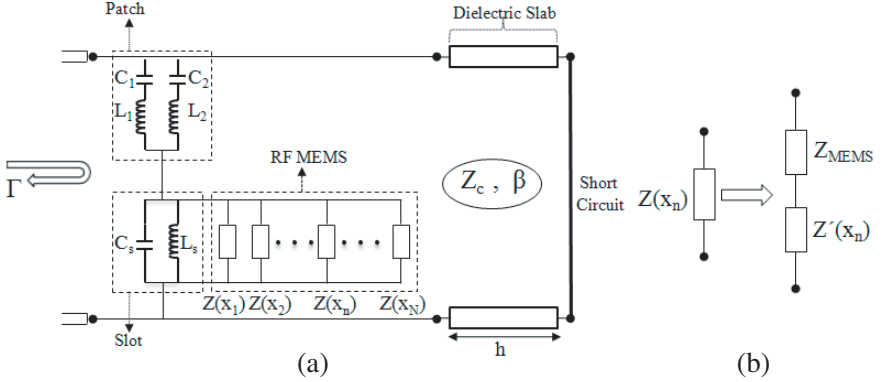
Figure 6. (a) Equivalent electrical circuit for a phase-shifter cell comprising of N MEMS; (b) Equivalent circuit model of the n-th MEMS within the slot (the total impedance $Z_{MEMS} + Z'$ depends on the ON/OFF state of the switch as well as its coordinate x_n inside the slot).

3. DESIGN AND OPTIMIZATION BASED ON THE EQUIVALENT CIRCUIT MODEL

The equivalent circuit model extracted above is used as a tool for designing and specifically for optimization of the phase shifter cell loaded with MEMS. By using this circuit model we find such phase-shifter configurations that have 360° phase range (i.e., 360° phase shift band width for a phase shifter cell) *at a single desired frequency*

with linear distribution of the selected phases and depend on the number N, the positions $x_1, x_2, x_3, \ldots, x_N$ and the state (ON/OFF) of the switches. To search out such phase shifter configurations out of thousands of the configurations is not possible by full wave simulations.

To find out the desired configurations, an algorithm based on the equivalent circuit model is developed, it selects the desired configurations from thousands of configurations (e.g., in case of three MEMS, the total configurations considered here are $70 * 69 * 68 = 328440$, the switch scanning step within the 7 mm slot is 0.1 mm) which fulfill the criteria of the 360° phase shift band width and the linearity among the desired selected phases. The selected configurations then directly give the optimized values of the two important design parameters for the phase shifter cell, i.e., the number N and the locations $x_1, x_2, x_3, \ldots, x_N$ of the MEMS used.

The algorithm was first applied in two switch case ($N = 2$) and it was observed that in this case, 360° phase range cannot be achieved within the desired frequency band (DC-14 GHz). Therefore a higher number ($N = 3, 4, 5, \ldots$) of switches was used and found that the required conditions are now easily fulfilled. By this algorithm, a lot of configurations consisting of 3 to 9 switches have been determined which satisfy the design requirements and proves the practicality of the equivalent circuit. However in a very few configurations the equivalent circuit results are not consistent with those of HFSS, such particular cases can be rejected *a posteriori* from the selection.

Because of limited space, only the results for just two configurations from 3-switch case ($N = 3$) are presented here. The total number of phases or commands for a configuration in case of 3 MEMS is eight ($2^N = 2^3 = 000 \ldots 111$, the symbols "1" and "0" represent ON and OFF state of the switch respectively). As per design requirements, we need such phase shifter configurations *at a single desired frequency within the operating frequency band* that cover linearly 360° phase range by four selected phases, that is to say a 90° phase shift between each state. By using the algorithm, we found many configurations that fulfill the above criteria; here the results of two configurations are given in Table 2 at 13 GHz. The results in case of both equivalent circuit model and HFSS are in very good agreement. The phase shift bandwidth is 360° for each phase shifter cell configuration.

In following, the Fig. 7 shows the response of Table 2(b) over the whole frequency range.

Table 2. Phase-shifts at $13\,\text{GHz}$, computed from the equivalent electrical circuit model and HFSS for phase-shifter cells loading by 3 RF-MEMS switches with (a) $x_1 = 2.25\,\text{mm}$, $x_2 = 3.2\,\text{mm}$, $x_3 = 6.65\,\text{mm}$, (b) $x_1 = 0.45\,\text{mm}$, $x_2 = 2.25\,\text{mm}$, $x_3 = 6.45\,\text{mm}$.

Command law	Observed Phase Shifts	Phase Φ_{EC} by equivalent circuit model	Phase Φ_{HFSS} by HFSS	Phase difference $\Phi_{EC} - \Phi_{HFSS}$
100	$0°$ (Reference)	$-164°$	$-175°$	$11°$
101	$87°$	$-77°$	$-80°$	$3°$
000	$179°$	$15°$	$19°$	$4°$
010	$271°$	$107°$	$100°$	$7°$

(a)

Command law	Observed Phase Shifts	Phase Φ_{EC} by equivalent circuit model	Phase Φ_{HFSS} by HFSS	Phase difference $\Phi_{EC} - \Phi_{HFSS}$
010	$0°$ (Reference)	$110°$	$104°$	$6°$
000	$91°$	$19°$	$21°$	$2°$
011	$186°$	$-76°$	$-67°$	$9°$
001	$274°$	$-164°$	$-174°$	$10°$

(b)
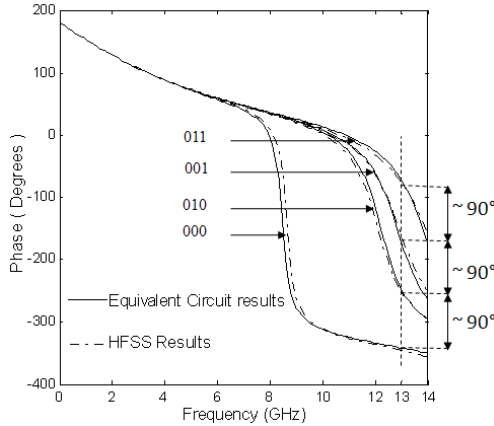
Figure 7. Comparison between equivalent circuit and HFSS results in three switch case under frequency range DC-14 GHz with $x_1 = 0.45\,\text{mm}$, $x_2 = 2.25\,\text{mm}$, $x_3 = 6.45\,\text{mm}$. The symbols "1" and "0" represent ON and OFF state of the switch respectively.

4. CONCLUSION

This paper presents a design and optimization tool in the form of an equivalent circuit for MEMS-controlled phase shifter cells. The results given by the equivalent electrical circuit have good agreement with full-wave electromagnetic simulations. This circuit model depends on the number, the ON/OFF state and the locations of the MEMS switches. Depending on these three parameters, it helps to search out such phase shifter configurations that provide 360° phase range with linear distribution of the selected phases.

REFERENCES

1. Legay, H., et al., "A steerable reflectarray antenna with MEMS controls," *IEEE Int. Phased Array Syst. Technol. Symp.*, 494–499, Oct. 14–17, 2003.

2. Hum, S. V., M. Okoniewski, and R. J. Davies, "Realizing an electronically tunable reflectarray using varactor diode-tuned elements," *IEEE Microwave and Wireless Components Letters*, Vol. 15, No. 6, 422–424, Jun. 2005.

3. Mossinger, A., R. Marin, S. Mueller, J. Freese, and R. Jakoby, "Electronically reconfigurable reflectarray with nematic liquid crystals," *Electron. Lett.*, Vol. 42, No. 16, 899–900, Aug. 2006.

4. Legay, H., et al., "Satellite antennas based on MEMS tunable reflectarrays," *Proc. Antennas and Propagation, EuCAP 2007*, 1–6, Nov. 11–16, 2007.

5. Perret, E., H. Aubert, and H. Legay, "Scale-changing technique for the electromagnetic modeling of MEMS-controlled planar phase shifters," *IEEE Trans. Microw. Theory Tech.*, Vol. 54, 3594–3601, Sept. 2006.

6. Dubrovka, R., J. Vazquez, C. Parina, and D. Moor, "Equivalent circuit method for analysis and synthesis of frequency selective surfaces," *IEE Proc. Microw. Antennas Propag.*, Vol. 153, No. 3, 213–220, Jun. 2006.

7. Hum, S. V., M. Okoniewski, and R. J. Davies, "Modeling and design of electronically tunable reflectarrays," *IEEE Transactions on Antennas and Propagation*, Vol. 55, No. 8, 2200–2210, Aug. 2007.

8. Legay, H., et al., "MEMS controlled linearly polarised reflectarray elements," *12th Int. Antenna Technol. Appl. Electromagn. Symp.*, Montréal, QC, Canada, Jul. 16–19, 2006.

9. Goldsmith, C. L., Z. Yao, S. Eshelman, and D. Denniston, "Performance of low-loss RF MEMS capacitive switches," *IEEE Microwave and Guided Wave Letters*, Vol. 8, No. 8, 269–271, Aug. 1998.

10. Peroulis, D., S. Pacheco, K. Sarabandi, and L. P. B. Katehi, "Tunable lumped components with applications to reconfigurable MEMS filters," *IEEE Int. Microw Symp. Digest*, Vol. 1, 341–344, May 20–25, 2001.

11. Nadarassin, M., H. Aubert, and H. Baudrand, "Analysis of planar structures by an integral approach using entire domain trial functions," *IEEE Trans. Microw. Theory Tech.*, Vol. 43, No. 10, 2492–2495, Oct. 1995.